ISSN 8755-6839

SCIENCE OF **TSUNAMI HAZARDS**

Journal of Tsunami Society International

Volume 40 Number 2 2021

NUMERICAL SIMULATION OF A CATASROPHIC EARTHQUAKE AND STRONG TSUNAMI OF APRIL 1, 2014 NEAR THE NORTHWESTERN PART OF THE CHILEAN COAST

Mazova R.Kh.[1,2], Moiseenko T.[1], Kurkin A.A.[1], Jorge Van Den Bosch F.[3], Gustavo Oses A.[3]

[1] Nizhny Novgorod State Technical University n.a. R.E. Alekseev, 24, Minin str., 603950 Nizhny Novgorod, Russia. e-mail address: Raissamazova@yandex.ru
[2]Moscow Institute of Physics and Technology (MIPT), Moscow Region, Russia
[3]Engineering Center Mitigation Natural Catastrophes Faculty of Engineering. Antofagasta. Chile. e-mail address: Jorge.VanDenBosch@uantof.cl; Gustavo.oses@uantof.cl

ABSTRACT

Catastrophic seismic events off the coast of Chile and the tsunami caused by them on April 1, 2014 north of Iquique with a magnitude of 8.2 are analyzed. Possible causes of moderate tsunami strength at a sufficiently large earthquake magnitude have been investigated. Within the framework of the keyboard block model of the subduction zone, based on the data on the localization of the main shock and aftershocks, the structure of the seismic source was selected. It was found that the computation results for the tsunami run-up noticeably exceed the observational data, which may be associated with the complex dynamics of the source. Comparison with the data of computations of other authors is performed.

Keywords: *tsunami, seismic and tsunami dangers, tsunamigenic earthquakes, tsunami waves, numerical simulation, Chilean coast.*

1. INTRODUCTION

One of the strongest recent earthquakes, followed by a strong tsunami, occurred on April 1, 2014 with a magnitude of M = 8.2 off the coast of northern Chile, 95 km northwest of Iquique. The tsunami hit the coast of Chile, causing significant damage. The epicenter of the mega-earthquake was in the subduction zone along the Peru-Chilean Trench, where the Nazca plate subducts under the South American plate at a convergence rate of about 65-80 mm / year. The nature of the generated tsunami waves in this zone, their propagation and behavior in the coastal zone have been analyzed in sufficient detail in the literature (see, e.g., (Brodsky and Lay, 2014; Catalan et al, 2015; Fritz et al., 2011; Hamlington et al., 2011; Hayes et al., 2012; Omira et al., 2016; Ramirez et al., 1997; Ruiz et al., 2016; Shrivastava et al., 2016; Zaytsev et al., 2016). Chile is in one of the most seismically active regions of the world - every day in northern Chile there are 15-30 weak shocks. Such a high level of seismic activity is associated with the geological structure of the northern part of Chile, where there is a deep-sea trench near the coast (up to 3000 m deep). However, there is also a very flat continental a slope that extends 150 km from the coast to the trench, forming a terrace.

The need to consider a more complex earthquake source for the Chilean subduction zone, adequate to the realization of aftershocks during an earthquake, was shown in our previous works (Mazova and Ramirez, 1999; Lobkovsky et.al., 2006). Historical records indicate that a series of catastrophic tsunamigenic earthquakes (Catalan et al., 2015; Omira et al., 2016) regularly occur off the coast of Chile. One of them occurred on August 13, 1868 with a maximum magnitude M = 8.5 in the southern region of Peru, when the earthquake source extended to the northern coast of Chile, near the city of Arica, which caused a strong tsunami, which later is referred to as the "tsunami in Arica". The epicenter of the earthquake was located less than 100 km of the coast, on the terrace of a deep-sea trench and in almost all coastal points where the tsunami was recorded, it began with the withdrawal of water from the coast, followed by a train of waves, in which the second wave was the most destructive. Tsunami waves caused by this earthquake reached a maximum coastal height of up to 21 m. The tsunami that occurred during the Chilean earthquake of 1868 reached the shores of New Zealand. Also, on May 10, 1877, a devastating earthquake with a magnitude of M = 8.8 occurred with a source off the northern coast of Chile, which was accompanied by a catastrophic tsunami. In the literature, this tsunami is referred to as the "Iquique tsunami". In the city of Iquique, the height of waves on the coast reached 4.8 m, and at various points on the coast of South America, tsunami waves hit the coast with a height of up to 24 m. Whole city blocks were washed away and destroyed.

In the 20th century, three catastrophic earthquakes accompanied by tsunamis also occurred on the coast of Chile, of which two occurred in central and northern Chile. Thus, on August 16, 1906, an earthquake with a magnitude of M = 7.8 occurred in the central and northern parts of the Chilean coast. The greatest damage was done to the city of Valparaiso. The maximum heights of tsunami waves along the coast reached 3.5 m. The runup to the coast proceeded moderately, in the form of coastal flooding. On May 22, 1960, a destructive mega-earthquake occurred with a source in the southern part of central Chile with a magnitude of M = 9.5. The maximum rise of water on the Chilean coast reached 25 m.

At the beginning of the 21st century, the strongest earthquakes occurred in the middle and northern parts of the Chilean coast. For example, on February 27, 2010, a catastrophic earthquake of magnitude $M = 8.8$ occurred off the coast of Chile, which caused a powerful tsunami (Pararas-Carayannis, 2010; Fritz et al., 2011; Hamlington et al., 2011; Hayes et al., 2012; Omira et al., 2016; Zaytsev et al., 2016). The source of the earthquake (35.909 ° S, 72.733 ° W) was in the sea at a depth of 35 km under the earth's crust, 17 km from the coastal settlements of Curanipe and Cobquecura, 90 km of the capital of Bio-Bio Concepcion, 150 km northwest of Concepcion and 63 km southwest of Cauquenes. An earthquake in Chile caused a powerful tsunami - twenty minutes after the earthquake, a sea wave two meters high struck the coast of Chile.

The strong earthquake on April 1, 2014 in northern Chile, off the Chilean coast, struck an area of a historic seismic gap called the gap in northern Chile (or the "Iquique gap"), which has experienced 5 major earthquakes every 114 years on average over the past 574 years, all with records of devastating tsunamis for cities in northern Chile and southern Peru, and some devastating impact on the Pacific Ocean. For the tsunamis that occurred in northern Chile in 1868 and 1877 (see above), there are tide gauge records of that time at Fort Point California USA, (see Fig. 1), where it can be seen other tsunamis that occurred in the north, central and southern parts of Chile where the largest tsunami from 1960 to 1922 stands out, the smallest registered by this old station.

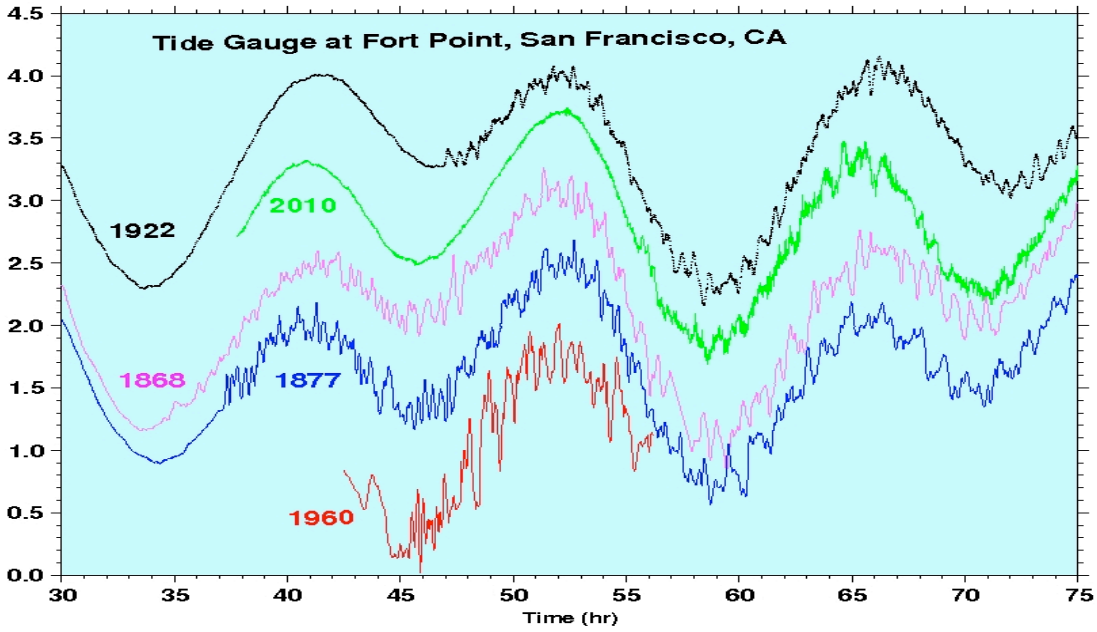

Fig. 1. Barrientos S. Wards S. 2008. (Private communication)

2. EARTHQUAKE AND TSUNAMI OF 01.04.2014 NEAR THE NORTHWESTERN PART OF THE CHILEAN COAST

It is important to note that the considered earthquake was preceded by an increasing seismicity and was directed from south to north (Internet resource ECDM_20140402_Chile_Earthquake). In this regard, during March 2014, shortly before the earthquake on April 1, 14 earthquakes-precursors occurred in the rupture zone; 3 earthquakes from 4.5º to 4.9º, 7 earthquakes from 5.1º to 5.8º and finally, very close to April 1, there were 4 earthquakes from 6.2º to 6.7º. This is likely a historical pattern of earthquakes preceding a major earthquake in this area.

This paper analyzes the catastrophic seismic event off the northern part of the Chilean coast on April 1, 2014. In the area of the city of Iquique, the epicenter of an earthquake with a magnitude of $M = 8.2$ was located in the region of 20.518° S and 70.498° W, a seismic fault called the northern Chilean or "Iquique seismic fault." Tsunami waves were recorded on the Chilean coast in cities: Pisagua - 1.7 m; Yunin - 1.7 m; Iquique - 1.6 m; Punta Negra - 1.6 m; Alto Hospice - 1.6 m; Chucumata - 1.3 m; Arica - 0.7 m. These data, as well as publicly available data on aftershocks, formed the basis of this study. Data on seismic activity in the Chilean subduction zone in 2014, leading to the occurrence of strong tsunamis that repeatedly hit the Chilean coast and leading to destruction are presented in Table 1.

Table 1. Earthquakes and tsunamis on the coast of Chile for 2014 event.

Date and time	Geographic coordinates	Magni-tudes	Region, contributed magnitudes and comments	Nearby cities
2014-04-03 02:43:14 UTC	20.518°S 70.498°W	7,7	Northern Chile. This earthquake is an aftershock of the $M = 8.2$ subduction zone earthquake that occurred April 1, 2014. The $M = 8.2$ event triggered a tsunami with measured heights near 2 meters along the northern Chile and southern Peru coasts. Since the $M = 8.2$ event, 47 aftershocks ranging from $M = 4.2$ to this M 7.8 event have occurred, including a M 6.4 on April 2.	1. 49km (30mi) SW of Iquique, Chile 2. 177km (110mi) N of Tocopilla, Chile 3. 227km (141mi) S of Arica, Chile 4. 269km (167mi) NW of Calama, Chile 5. 509km (316mi) SSW of La Paz, Bolivia
2014-04-01 23:57:57 UTC	19.898°S 70.924°W	6,9	Northern Chile.	1. 89km (55mi) WNW of Iquique, Chile 2. 170km (106mi) SSW of Arica, Chile 3. 221km (137mi) SSW of Tacna, Peru 4. 253km (157mi) S of Ilo, Peru 5. 476km (296mi) SW of La Paz, Bolivia
2014-04-01 23:46:46 UTC	19.642°S 70.817°W	8,2	Northern Chile. The April 1, 2014 $M = 8.2$ earthquake in northern Chile occurred as the result of thrust faulting at shallow depths near the Chilean coast. The April 1 earthquake occurred in a	1. 95km (59mi) NW of Iquique, Chile 2. 139km (86mi) SSW of Arica, Chile 3. 190km (118mi) SSW of Tacna, Peru

			region of historic seismic quiescence – termed the northern Chile or Iquique seismic gap. Historical records indicate a M = 8.8 earthquake occurred within the Iquique gap in 1877, which was preceded immediately to the north by an M = 8.8 earthquake in 1868.	4. 228km (142mi) SSE of Ilo, Peru 5. 447km (278mi) SW of La Paz, Bolivia
2014-03-16 21:16:30 UTC	19.925°S 70.628°W	6,7	Northern Chile. This earthquake is considered the last precursor of the 8.2º major earthquake on April 1, 2014 in this area (Internet resource ECDM_20140402_Chile_ Earthquake).	1. 60km (37mi) WNW of Iquique, Chile 2. 164km (102mi) SSW of Arica, Chile 3. 216km (134mi) S of Tacna, Peru 4. 244km (152mi) N of Tocopilla, Chile 5. 460km (286mi) SW of La Paz, Bolivia

3. SEISMIC SOURCE MODEL FOR THE APRIL 1, 2014 CHILEAN EARTHQUAKE

Figure 2 shows the localization of the source of the April 1, 2014 earthquake in northern Chile and aftershocks in the next 2 days after the main shock, as well as the data of the tide gauge in Patach. The epicenter of the earthquakes was in the region of 20.518 ° S and 70.498 ° W. Tsunami waves have been recorded on the Chilean coast in a number of cities (see above).

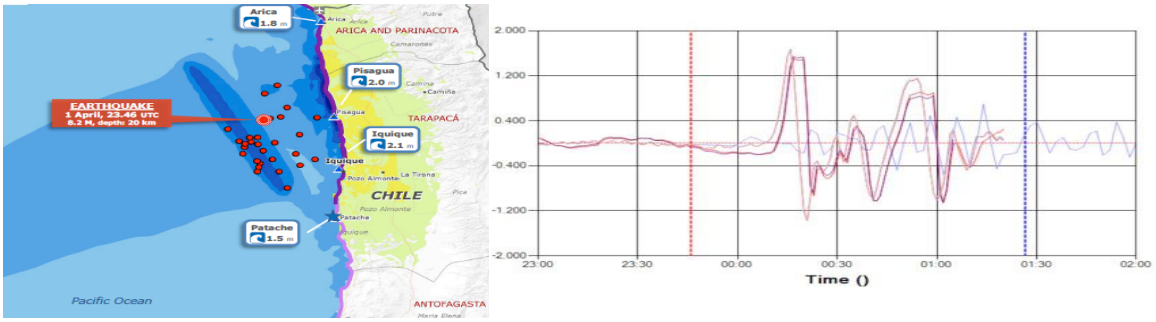

a) b)

Fig. 2. a) Localization of the earthquake source and the location of aftershocks in the next 2 days after the main shock; b) data from a tide gauge in Patache (Internet resource ECDM_20140402_ Chile_Earthquake [20]).

In this paper, to carry out numerical modeling of this earthquake, a three-block seismic source with a size of 110 × 230 km is considered. (Fig. 3). The area of the source is 25300 km^2; the height of the maximum vertical rise is 4 m (see Table 2). If we take into account the localization and time of aftershocks, then the shape of the source will have a more complex form (see Fig.3). In accordance with the seismic process in the source, the movement of the keyboard blocks is defined in Table 2.

Table 2. Characteristics of simulated sources (Scenario 1).

Block number	1	2	3
Heights (m)	2	4	1
Movement start time (s)	90	0	40
Movement final time (s)	120	40	90

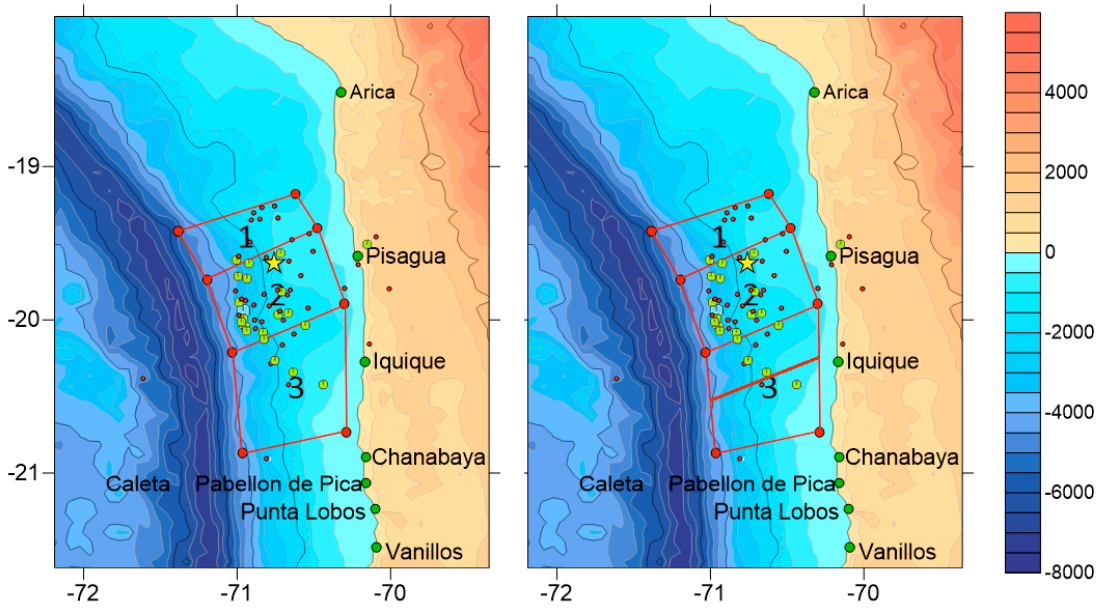

a) *b)*

Fig. 3. The shape of the earthquake source of April 1, 2014: a) for 3-block seismic source (Scenario 1); for 4-block seismic source (Scenario 2).

4. MATHEMATICAL STATEMENT OF THE PROBLEM

To simulate the generation and propagation of tsunami waves from an earthquake, a scenario was adopted that was selected according to the direction of seismic activity. For numerical simulation of a tsunami from a seismic source located along the Chilean coast, a part of the Pacific Ocean basin in the square of 600-900 E. and 50-400 S was used. To describe the process of wave generation and propagation in accordance with the assumptions made above, a system of nonlinear shallow water equations is used (see, for example, (Mazova et al., 2006; Voltsinger et al., 1989).

$$\begin{cases} \vec{U}_t + \vec{U} \cdot grad\ \vec{U} + g \cdot grad\,\eta = 0 \\ \eta_t + div\left((H + \eta - B)\vec{U}\right) = B_t \end{cases} \qquad \vec{U} = \begin{pmatrix} u \\ v \end{pmatrix}$$

Here the functions u and v are the velocities of the water particles; g is the acceleration of gravity, $B(x, y, t)$ is a function that describes the law of motion of the basin bottom when

simulating the dynamics of the displacement of the Earth's crust in the earthquake source (within the framework of the key-block model of the earthquake source). Under this simulation a modernized finite-difference scheme (Sielecki and Wurtele, 1970) (see, for example, (Lobkovsky et al., 2019)) was used.

5. RESULTS OF NUMERICAL SIMULATION

Figure 4 shows the characteristic moments during the generation of the tsunami source by the selected seismic source for three points in time corresponding to the movement of three key blocks.

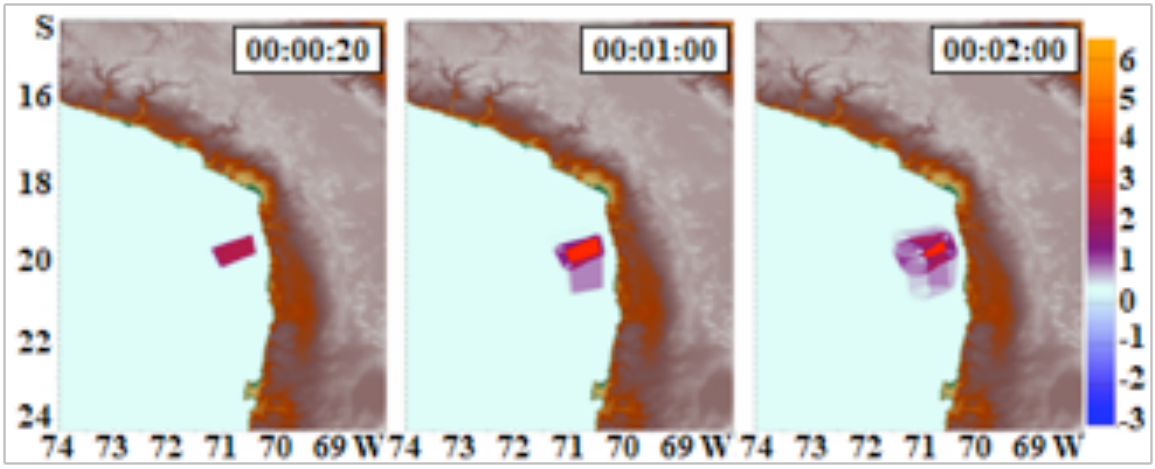

Fig. 4. The generation of a tsunami source

Figure 5 shows the process of wave propagation over the water area for 9 points in time. For this formulation of the problem, the process of wave propagation is considered on a part of the Pacific Ocean: along the central part of the Chilean coast. For this scenario, Fig. 6 shows the distribution of the maximum wave heights over the computed water area. It can be seen that the highest wave heights are localized in the area of the earthquake source, while along the coast, wave heights of 5-6 m are possible. Analysis of the results shows that the highest wave heights were recorded in the central part of the water area.

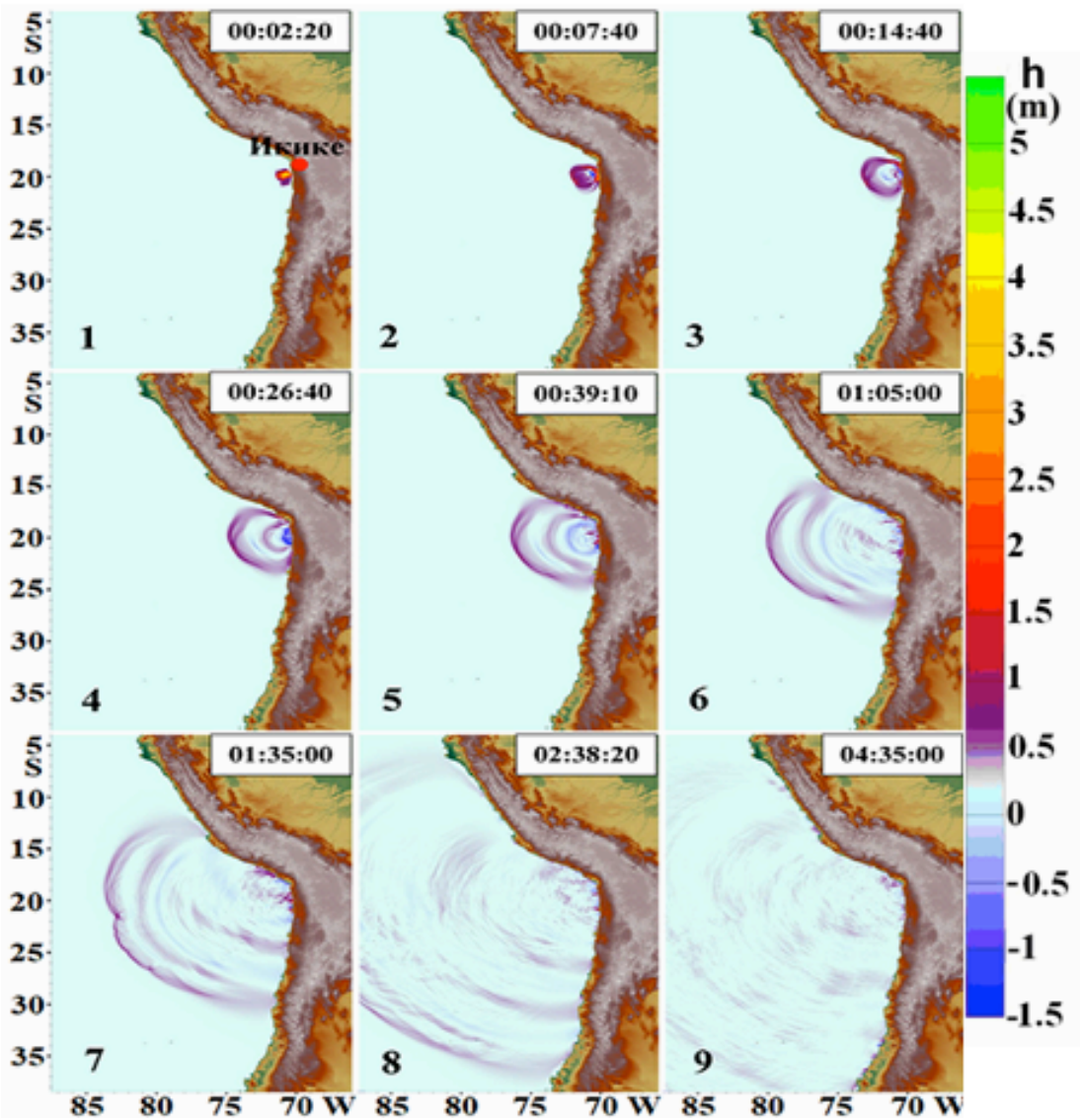

Fig. 5. Propagation of a tsunami waves by a 3-block seismic source for the 9 time moments (Scenario 1).

Figures 7 and 8 show a histogram for central Chile and southern Peru. It is clearly seen that the maximum heights for the central part of Chile reach 6m, and for the southern coast of Peru up to 5m.

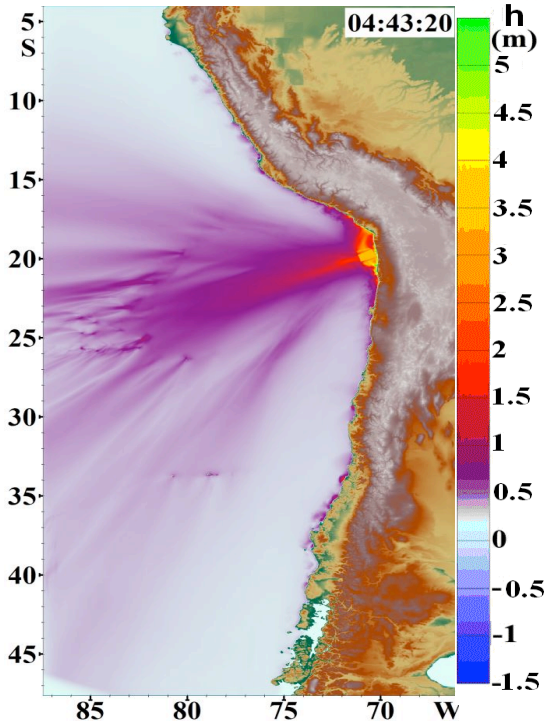

Fig. 6. Distribution of maximum wave heights for a part of this water area according to the results of numerical simulation under Scenario 1.

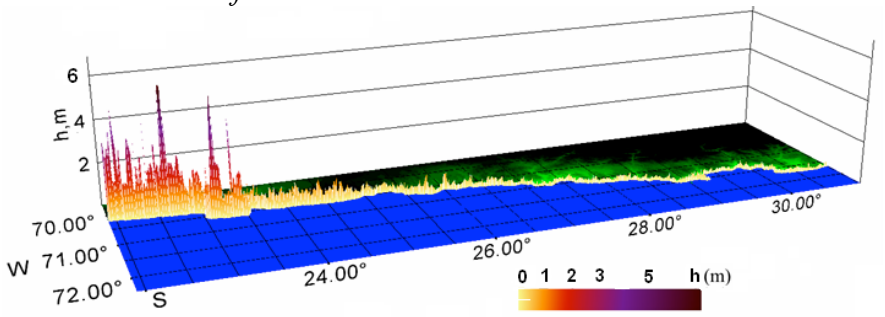

Fig. 7. 3D histogram for central part of Chile (Scenario 1).

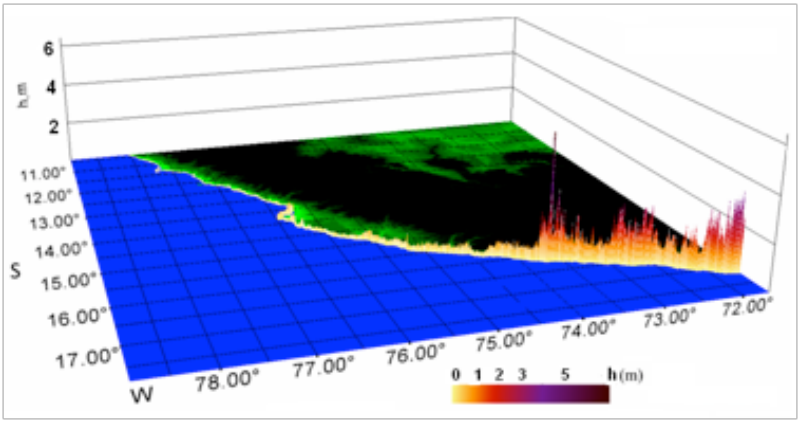

Fig. 8. 3D histogram for southern coast of Peru (Scenario 1).

Table 3 shows the computed data on the height of tsunami waves at the 10-meter isobath along the Chilean coast in the area of the computational domain. It can be seen that with the selected geometry and structure of the source, as well as for the given dynamics of the key blocks, the greatest runup value is obtained for pp. Iquique, Pisagua, Arica, and Tocopilla, and with distance from the source, the runup value decreases, reaching 1.6 m for Taltal and 0.8 m for Paposo on both sides of the source.

Table 3. Results of numerical simulation of runup heights (Scenario 1)

Point	Field-data heights , m	Numerical simulation, m
Matarani (72.11°W 17.02°S)	0.6	1.6
Arica (70.29°W 18.47°S)	1.65	3.7
Caleta Camarones (70.26°W 19.18°S)	-	-
Pisagua (70.2°W 19.6°S)	2.3	4.3
Iquique (70.1°W 20.2°S)	1.8	5.2
Patache (70.2°W 20.8°S)	1.7	-
Tocopilla (70.19°W 22.08°S)	1.5	3.2
Mejillones (70.45°W 23.1°S)	0.7	1.6
Antofagasta (70.39°W 23.65°S)	0.35	1.1
Paposo (70.46°W 25.01°S)	0.35	0,8
Taltal (70.48°W 25.4°S)	0.35	1,1
Chanaral (71.58°W 29.03°S)	0.5	-

To correct the results obtained, a numerical simulation was performed for a four-block earthquake source (see Fig. 3b).

Table 4. Characteristics of simulated sources (Scenario 2).

Block number	**1**	**2**	**3**	**4**
Heights (m)	**1.2**	**1.6**	**1.3**	**1.5**
Movement start time (s)	**30**	**0**	**60**	**100**
Movement final time (s)	**60**	**30**	**100**	**120**

Figure 9 shows three characteristic time moments under generation of the tsunami source by the selected seismic source.

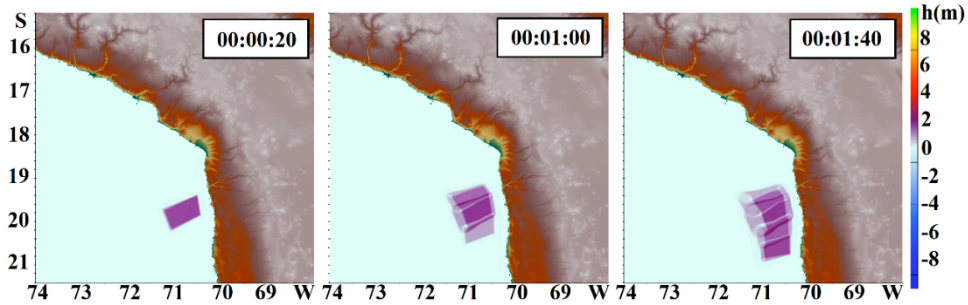

Fig. 9. The generation of a tsunami source.

For this scenario, Fig. 10 shows the distribution of the maximum wave heights over the computed water area.

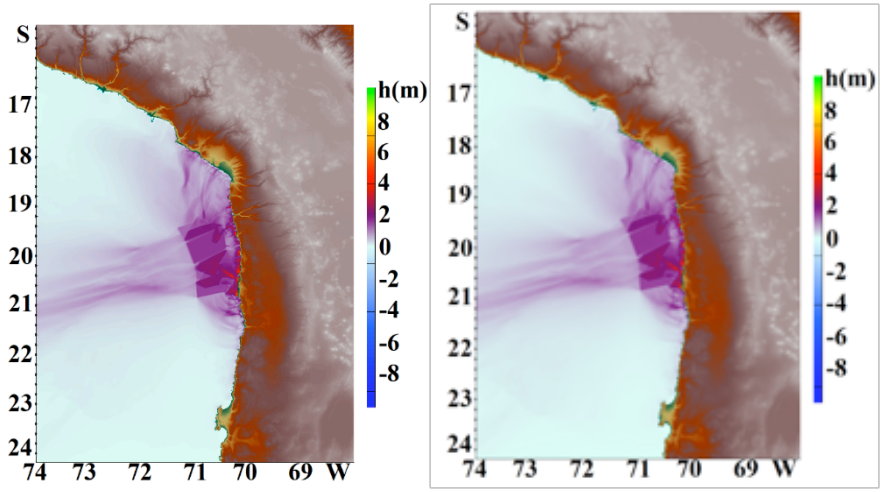

Fig. 10. Distribution of maximum wave heights for a part of this water area according to the results of numerical simulation under Scenario 2.

Figure 11 shows a 2D histogram for central Chile. It is clearly seen that the maximum heights for the central part of Chile are somewhat higher than 5m.

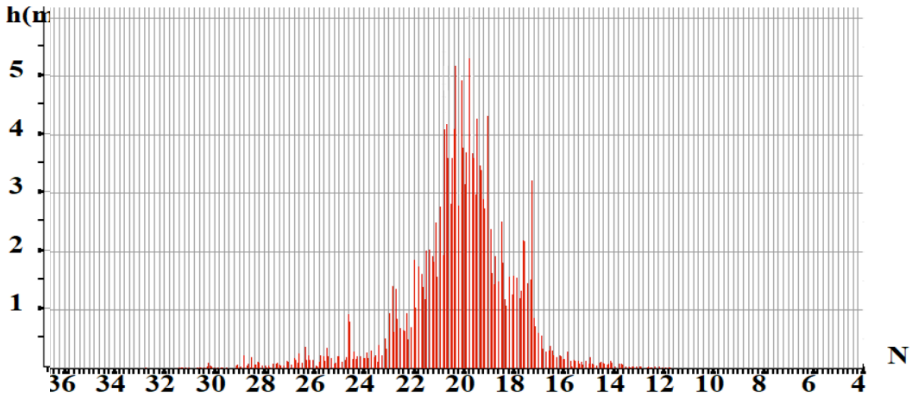

Fig. 11. 2D histogram for central Chile (Scenario 2).

The computation results for Scenario 2 and comparison with field data and computations for Scenario 1 are shown in Table 5. It can be seen that with the chosen geometry and structure of the source, as well as for the dynamics of the key blocks for Scenario 2, there is a good agreement with the field data. The deviation from the field data is available only for the Pisagua and Iquique points, which is obviously related to the shape of the source.

Table 5. Comparison of field-data and computed heights

№	Points	Field-data heights , m	Numerical simulation, m (Scenario 1)	Numerical simulation, m (Scenario 2)
1	**Matarani** (72.11°W 17.02°S)	0.6	1.6	0.6
2	**Arica** (70.29°W 18.47°S)	1.65	3.7	1.8
3	**Caleta Camarones** (70.26°W 19.18°S)	-	-	3.48
4	**Pisagua** (70.2°W 19.6°S)	2.3	4.3	3,5
5	**Iquique** (70.1°W 20.2°S)	1.8	5.2	2,8
6	**Patache** (70.2°W 20.8°S)	1.7	-	1.95
7	**Tocopilla** (70.19°W 22.08°S)	1.5	3.2	0.7
8	**Mejillones** (70.45°W 23.1°S)	0.7	1.6	0.35
9	**Antofagasta** (70.39°W 23.65°S)	0.35	1.1	0.3
10	**Paposo** (70.46°W 25.01°S)	0.35	-	0.2
11	**Taltal** (70.48°W 25.4°S)	0.35	-	0.2
12	**Chanaral** (70.64 °W 26.35 °S)	0.5	-	0.37

6. DISCUSSION

The results comparing the obtained computations (Scenario 1) with empirical data and computations by other authors are shown in Fig.9 and Table 4. Figure 9 shows a comparison of the computed results with field data and data from (Catalan et.al, 2015). It can be seen that the histogram of the distribution of the maximum wave heights is close to the empirical data in terms of the nature of the distribution, the wave heights are closest in the interval along the coast between 23_S and 18_S, but the computation data for the chosen scenario (Table 3) at some points is significantly higher than the field data (Table 4, column 1).

The data given in Table 3, field data, and data from (Catalan et.al, 2015) on the Chile earthquake and tsunami, 2014 are summarized in Table 4. It can be seen that the data on numerical simulation given in Scenario 1 are consistent with real data, taking values close to empirical data only in a limited number of points. This can be explained by the fact that the dynamics of blocks in the source was determined primarily by the nature of bottom bathymetry with aftershocks of the first day of the earthquake. As can be seen from the Table, the computed heights in the cited work (Catalan et.al, 2015) are significantly higher than the observational ones. It should be noted here that the observed runup heights themselves in this case are rather moderate for such strong earthquakes.

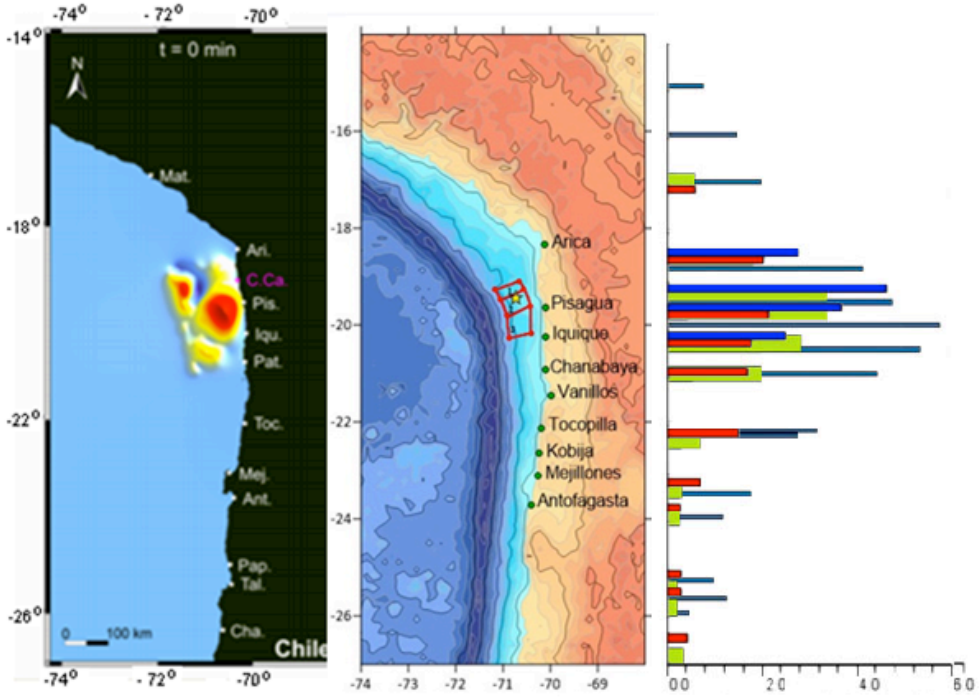

Fig. 9. Comparison of computed and natural data for two model of seismic source for Chilean 2014 earthquake and tsunami event. Red lines – natural data; blue lines – data from work (Catalan et.al.,2015); grey lines – computation on Scenario 1; green lines – computation on Scenario 2.

A comparative analysis with the data of works (Catalan et al., 2015; Omira et al., 2016; Ruiz et al., 2016; Shrivastava et al., 2016; Zaytsev et al., 2016) shows that the facts given in these works are somewhat contradictory, and there is little reliable information, which did not allow us to set a more adequate dynamics of blocks in the earthquake source. In (Ruiz et al., 2016) it is noted that, depending on the model of the seismic source for a given earthquake, numerical modeling gives the values of the maximum wave heights in the range from 5 to 40 m, and the average values lie in the region of 10 m, which is significantly higher than the observed values.

Table 4. Comparison of field-data and computed heights

Point	Field-data heights , m	Computed heights, m [Catalan et.al., 2015]	Numerical simulation, m (Scenario 2)
Matarani (72.11°W 17.02°S)	0.6	-	0.6
Arica (70.29°W 18.47°S)	1.65	2.9	1.8
Caleta Camarones (70.26°W 19.18°S)	-	4.7	3.48
Pisagua (70.2°W 19.6°S)	2.3	3.7	3,5
Iquique (70.1°W 20.2°S)	1.8	2.6	2,8
Patache (70.2°W 20.8°S)	1.7	-	1.95
Tocopilla (70.19°W 22.08°S)	1.5	-	0.7
Mejillones (70.45°W 23.1°S)	0.7	-	0.35
Antofagasta (70.39°W 23.65°S)	0.35	-	0.3
Paposo (70.46°W 25.01°S)	0.35	1	0.2
Taltal (70.48°W 25.4°S)	0.35	0,5	0.2
Chanaral (71.58°W 29.03°S)	0.5	-	0.37

7. CONCLUSIONS

As previously predicted by a number of authors (see, for example, (Mazova and Soloviev, 1994)), seismic activity along the perimeter of the Pacific Ocean will significantly increase by the end of the 20th - beginning of the 21st centuries. Indeed, there was a series of catastrophic earthquakes accompanied by a tsunami: in the Indian Ocean near Sumatra on December 26, 2004 with a magnitude of 9.1, an earthquake and tsunami on November 15, 2006 in the Kuril-Kamchatka region, a catastrophic earthquake with a magnitude of 8.8, which occurred in middle part of Chile on February 27, 2010, a tsunamigenic catastrophic earthquake in Japan on March 11, 2011 with a magnitude of 9.2 and the last event - a strong earthquake and tsunami in northern Chile in April 1 January 2014 with a magnitude of 8.2. The nature of the generated tsunami waves for each of these events, their propagation and behavior in the coastal zone have been analyzed in sufficient detail in the literature (see above).

As follows from the works on the analysis of the ratio of the earthquake magnitude and tsunami run-up height, a complex earthquake source without taking into account the geodynamics in the seismic source and taking into account the effects of the coastal zone, gives higher heights than a monoblock (see, for example, Kurkin et al., 2004; Lukhnov et al., 2006; Tyatyushkina et al., 2020; Yalciner et al., 2007; Zaitsev et al., 2020). This conclusion also follows from a number of recent works (Ruiz et al., 2015, Catalan et al., 2016, Omira et al., 2016; Zaytsev et al., 2016). For example, in (Ruiz et al., 2015), the potential possibility of a new earthquake in a large seismic gap along northern Chile was considered, where the Pisagua earthquake occurred on April 1, 2014, which destroyed the middle segment of this gap, leaving the southern and northern segments not destroyed. So this region has a large area that can generate an earthquake with $M > 8.5$ and a strong tsunami. In their numerical modeling, they took a magnitude $M = 9$ in northern Chile and calculated the vertical co-seismic static displacement, adding up the elementary "sections". The paper analyzes a number of chaotic fault models, taking into account the nonplanar geometry of the fault in northern Chile. Numerical results in some cases show the maximum run-up of 30-40 m. Instead, the minimum run-up coincides with homogeneous (monoblock) models of the order of 4 m. In the latter case, there is an underestimation by a factor of 6. Analysis shows that models with a lot of slip near the trough are likely to produce higher runups than other scenarios. In (Catalan et al., 2016), a numerical simulation of the tsunami on April 1, 2014, caused by an earthquake with a magnitude $M =$ 8.2 near the coast of northern Chile, was carried out. The analysis of the characteristics of this tsunami was carried out on the basis of a comparison of the results of numerical simulation with field data. Despite the large magnitude of the earthquake, the tsunami was moderate, with a relatively uniform distribution of runup - the runup peak was 4.6 m. This is explained by the authors with the concentration of the maximum slip achieved at an intermediate depth on the fault, resulting in a rapid decay of the tsunami energy. The temporal evolution of a tsunami is changing - there are places where tsunami energy is conserved, while in other places tsunami energy increases over time after an earthquake. The authors believe that this is the result of the interaction of long-period standing oscillations and the activity of a trapped edge wave controlled by the inner slopes of the shelf.

In (Omira et al., 2016; Zaytsev et al., 2016), the relationship between the generation and propagation of tsunamis in the near-field zone and coseismic deformation was investigated for three recent (2010, 2014 and 2015) earthquake and tsunami events in the deep-water region of Peru-Chilean Trench. These three earthquakes were found to be due to faults with important extensions under the continent, which result in tsunamis with short wavelengths, relative to the width of the faults involved, and with reduced initial potential energy. In addition, the presence of the Chilean continental margin, which includes a shallow bathymetry shelf and a continental slope, inhibits tsunami propagation and coastal impact. All these factors contribute to the concentration of the local impact, but may, on the other hand, reduce the effects of the tsunami in the far-field zone from earthquakes along the Peru-Chile Trench.

Thus, the study carried out in this work confirms the need to consider the source of an earthquake of a more complex shape, taking into account the geodynamic processes in the source, adequate implementation of the aftershock process during an earthquake and taking into account the effects of the coastal zone, as was shown in our previous works (Lobkovsky et al., 2006; Mazova et al., 2014, Lobkovsky et al., 2017, Lobkovsky et al., 2019, Lobkovsky et al., 2021).

ACKNOWLEDGEMENTS

The authors acknowledge the funding of this study provided by grant of President of the Russian Federation for the state support of Leading Scientific Schools of the Russian Federation (Grant No. NSH-2485.2020.5).

REFERENCES

Brodsky E.E. and Thome Lay, (2014) *Recognizing Foreshocks from the 1 April 2014 Chile Earthquake* // Science. 344, 700.

Catalan P.A. et al. (2015) *The April 01, 2014, Pisagua Tsunami: Observations and Modeling* // American Geophysical Union.

Dunbar P., Stroker K., Heather McCullough (2010). *Do the 2010 Haiti and Chile earthquakes and tsunamis indicate increasing trends?* // Geomatics, Natural Hazards and Risk 1 95-114.

Fritz H.M. et al. (2011) *Field Survey of the 27 February 2010 Chile Tsunami* // Pure Appl. Geophys. 168 , 1989–2010

Hamlington, B.D., R.R. Leben, O.A. Godin, J.F. Legeais, E. Gica, and V.V. Titov: (2011) *Detection of the 2010 Chilean tsunami using satellite altimetry*. Nat. Hazards Earth Syst. Sci., 11, doi: 10.5194/nhess-11-2391-2011, 2391–2406.

Hayes G.P. et al. (2012) *Slab1.0: A three-dimensional model of global subduction zone geometries* // J. Geophys. Res.,. 117, B01302, Internet resource ECDM_20140402_ Chile_Earthquake.

Kurkin A.A., Zaitsev A.I., Yalchiner A., Pelinovsky E.N. (2004) *Modified computer complex "Tsunami" for assessing the risks associated with tsunami* // Izvestia of the Academy of Engineering Sciences named after A.M. Prokhorov. V. 9. P. 88-100.

Lobkovsky L.I. Geodynamics of spreading, subduction and two-level plate tectonics zones // Nauka Press, Moscow, USSR, 1988.

Lobkovsky L.I., Baranov BV. Keyboard model of strong earthquakes in island arcs and active continental margins // Doklady of the Academy of Sciences of the USSR. V. 275. № 4. P. 843-847. 1984.

Lobkovsky L.I., Nikishin A.M., Khain V.E. Current problems of geotectonics and geodynamics // Nauchnyi Mir Press, Moscow, Russia, 2004.

Lobkovsky, L. I., Mazova, R. Kh, Kataeva, L Yu., & Baranov, B.V. (2006) Generation and propagation of catastrophic tsunami in the basin of Sea of Okhotsk. Possible scenarios, // Doklady, V.410, 528–531.

Lobkovsky L., I.Garagash, B.Baranov, R.Mazova, N.Baranova. (2017) *Modeling Features of Both the Rupture Process and the Local Tsunami Wave Field from the 2011 Tohoku Earthquake* // Pure Appl. Geophys. V.174, P.3919-3938, doi:10.1007/s00024-017-1539-5 p.1-20.

Lobkovsky L.I., I. A. Garagash, R. Kh. Mazova. (2019) *Numerical simulation of tsunami waves generated by the underwater landslide for the Northern Coast of the Black Sea (Dzhubga Area*) // Geophys. J. Int. V.218, P.1298–1306, https://doi.org/10.1093/ gji/ ggz221).

Lukhnov A.O., Chernov A.G., Kurkin A.A., Polukhina O.E. (2006) *Problems of creating a hardware-software complex for studying the hydrodynamics of the shelf zone..*// Izvestiya of the Academy of Engineering Sciences. A.M. Prokhorov. V.18, P. 120-123.

Mazova R.Kh. Soloviev S.L.. (1994) *On influence of sign of leading tsunami wave on runup height on the coast* // Sci.Tsunami Hazards V.12, P. 25-31.

Mazova R.Kh, Ramirez J.F. (1999) *Tsunami waves with an initial negative wave on the Chilean coast //* Natural Hazards V.20, P83-92.

Mazova R.Kh., B.V. Baranov, L.I. Lobkovsky, N.A. Baranova, K.A.Dozorova, O.N. Chaykina. (2014) *Numerical Model Study of Possible Earthquake – Generated Tsunami in Komandorsky Seismic Gap, Western Aleutian Island Arc* // Sci.Tsunami Haz. V.32, 131–155.

Mendosa Carlos, (USGS) "Basic Seismology for Geotechnics, Construction and Risks", course. Faculty of Engineering. University of Antofagasta. 6-7 Nov 1997. (private communication).

Murty T.C. Seismic Sea Waves: Tsunami // Dept. of Fisher. and the Environ., FMS: Ottawa Canada, 1977

Omira R. et al. (2016) *Tsunami Characteristics Along the Peru–Chile Trench: Analysis of the 2015 Mw8.3 Illapel, the 2014 Mw8.2 Iquique and the 2010 Mw8.8 Maule Tsunamis in the Near-field* // Pure Appl. Geophys. V.173, 1063–1077

Pararas-Carayannis G. *The earthquake and tsunami of 27 February 2010 in Chile - Evaluation of source mechanism and of near- and far-field tsunami effects* // Sci.Tsunami Hazards 29 (2010) 96-126.

Pelinovsky, E.N., Soloviev, S.L., Mazova, R.Kh. *Statistical data on the character of the run-up of tsunami waves* // Oceanology 23 (1983) 932-937.

Pelinovsky E.N. & Mazova R.Kh., 1992, *Exact analytical solution of nonlinear problems of tsunami wave runup on slopes with different profiles* // Natural Hazards, 6, 227-249

Pritchard M.E., M. Simons, P. A. Rosen, S. Hensley and F. H. Webb. (2002) *Co-seismic slip from the 1995 July 30 Mw =8.1 Antofagasta, Chile, earthquake as constrained by InSAR and GPS observations* // Geophys. J. Int. V.150, 362–376.

Ramirez, J. Titichoca, H. Lander J. and Whiteside L. (1997) *The minor destructive tsunami occurring near Antofagsta, northen Chile, july 30 1995*, Science of Tsunami Hazards, V.15, No. 1. Hawaii USA.

Ruiz J.A. et al. (2015) *Numerical simulation of tsunami runup in northern Chile based on non-uniform k22 slip distributions* // Nat Hazards 79:1177–1198.

Shrivastava M.N. et al. *Earthquake segmentation in northern Chile correlates with curved plate geometry* // Sci.Rep.

Sielecki, A., and M. Wurtele, (1970) The numerical integration of the nonlinear shallow water equations with sloping boundaries // J.Comput. Phys., V.6, P.219, doi:10.1016/0021- 9991(70)90022-7.

Tyatyushkina E., Kozelkov A., Kurulin V., Plygunova K., Utkin D., Kurkin A., Pelinovsky E. (2020) *Verification of the Logos software package for tsunami simulations* // Geosciences (Switzerland). V. 10. № 10. P. 1-28.

Urzúa U. Luis "Arica Puerta Nueva" 3° Edición. Editorial Andrés Bello. Santiago Chile. 1969

Yalciner A.C., Ozer C., Karakus H., Ozyurt G., Pelinovsky E., Zaitsev A., Kurkin A. (2007) *Modeling and visualization of tsunamis: Mediterranean examples* // In: Tsunami and Nonlinear Waves. P. 273-283.

Voltsinger N.E., Klevanny K.A. & Pelinovsky E.N., 1989, *Long-Wave Dynamics of Coastal Zone*, Gidrometeoizdat, Leningrad, USSR, (in Russian).

Zaytsev O. et al. (2016) *A Comparative Analysis of Coastal and Open-Ocean Records of the Great Chilean Tsunamis of 2010, 2014 and 2015 off the Coast of Mexico* // Pure Appl. Geophys. V.173, 4139–4178.

Zaytsev A.I., Kurkin A.A., Pelinovsky E.N., Yalçıner A. (2020) *The Use of the NAMI-DANCE Computational Complex on the Problem of Tsunami Waves* // J.Appl. Mech. and Tech. Phys. V.61. No. 7. P. 1140–1152.